



Neurofilaments are Flexible Polymers That Often Fold and Unfold, But They Move in a Fully Extended Configuration

Nicholas J. Taylor,^{1,2} Lina Wang,¹ and Anthony Brown^{1*}

¹Department of Neuroscience, Wexner Medical Center, Ohio State University, Columbus, Ohio

²Undergraduate Biomedical Science Honors Program, School of Biomedical Science, Wexner Medical Center, Ohio State University, Columbus, Ohio

Received 6 April 2012; Revised 8 May 2012; Accepted 9 May 2012
Monitoring Editor: Peter Baas

Time-lapse imaging of neurofilaments in axons of cultured nerve cells has demonstrated that these cytoskeletal polymers move along microtubule tracks in both anterograde and retrograde directions, powered by microtubule motors. The filaments exhibit short bouts of rapid intermittent movement interrupted by prolonged pauses, and the average velocity is slow because they spend most of their time pausing. Here, we show that axonal neurofilaments are also very flexible and frequently exhibit complex and dynamic folding and unfolding behaviors while they are pausing. Remarkably, however, when the filaments move in a sustained manner, we find that they always adopt an unfolded, that is, fully extended configuration, and this applies to movement in both anterograde and retrograde directions. Given the flexibility of neurofilament polymers and the apparent ease with which they can fold back on themselves, the fact that they move in a fully extended configuration suggests that moving neurofilaments may be pulled from their leading end. Thus, we speculate that motors may bind to the leading ends of neurofilaments polymers during both anterograde and retrograde motion.

© 2012 Wiley Periodicals, Inc

Key Words: neurofilament, intermediate filament, axonal transport, motor protein, cytoskeleton, axon

Additional Supporting Information may be found in the online version of this article.

Lina Wang's present address is Department of Pathology, School of Medicine, University of California San Diego, La Jolla, California 92093.

*Address correspondence to: Dr. Anthony Brown, Department of Neuroscience, The Ohio State University, Rightmire Hall, 1060 Carmack Road, Columbus, Ohio 43210, USA.
E-mail: brown.2302@osu.edu

Published online 12 June 2012 in Wiley Online Library (wileyonlinelibrary.com).

Introduction

Neurofilaments, which are the intermediate filaments of nerve cells, are transported along axons in the slow components of axonal transport at average rates on the order of millimeters or tenths of a millimeter per day [Lasek et al., 1992; Perrot et al., 2008]. Live-cell imaging studies on neurofilaments in cultured nerve cells using neurofilament proteins tagged with green fluorescent protein (GFP) have shown that these polymers actually move rapidly, approaching the speed of membranous organelles, but the average rate is slow because the rapid movements are interrupted by prolonged pauses [Brown, 2000; Wang et al., 2000].

It is now clear that the long-range movements of neurofilaments in axons occur along microtubule tracks [Prahlaad et al., 2000; Shah et al., 2000; Francis et al., 2005]. Several lines of evidence suggest that the retrograde motor is dynein [Shah et al., 2000; Helfand et al., 2003; Wagner et al., 2004; He et al., 2005] and that the anterograde motor is one or more of the kinesin-1 isoforms, including kinesin-1A [Yabe et al., 2000; Helfand et al., 2003; Xia et al., 2003; Jung et al., 2005; Uchida et al., 2009]. It is also clear that the activities of these opposing motors are coupled in some way because disruption of either dynein or kinesin-1A motors impairs movement of neurofilaments in both directions [Uchida et al., 2009]. However, while there is some evidence for an interaction of dynein and kinesin-1 with neurofilaments [Shah et al., 2000; Yabe et al., 2000; Wagner et al., 2004; Jung et al., 2005], nothing is known about the number of motors that bind each neurofilament, what subunits or sites they bind to, and whether the interaction is direct or indirect.

During the past 10 years, we have acquired time-lapse movies of many hundreds if not thousands of neurofilaments in the axons of a variety of different types of cultured neurons and we have consistently been struck by the flexibility of these polymers and the fact that they often fold and unfold in a complex and dynamic manner. To learn more about this folding behavior, we performed

length measurements and axial intensity profile analyses on moving and pausing neurofilaments in time-lapse movies of axons of cultured cortical neurons from neonatal mice. The diffraction-limited width of neurofilaments in our fluorescence images precludes direct visualization of the fold configuration in most cases. However, we found that folding can be detected reliably because it results in a local increase in the fluorescence intensity along the filament at the site of the fold, accompanied by a corresponding decrease in apparent filament length. Using this approach, we found that axonal neurofilaments often fold while they are pausing, but remarkably, when the filaments move in a sustained manner they invariably straighten out and adopt an unfolded, that is, fully extended, configuration. This has potentially intriguing implications for the mechanism by which motors interact with these cytoskeletal cargos.

Materials and Methods

Cell Culture and Transfection

Neurons were dissociated from the cerebral cortices of neonatal mice and cultured on glass coverslips with an astrocyte feeder layer according to the sandwich technique of Kaech and Banker [2006], as described by Wang and Brown [2010]. To prepare glial cultures, the cerebral cortices of 3–5 P0 mouse pups were dissociated in phosphate buffered saline (PBS; GIBCO Life Technologies, Grand Island, NY) containing 0.25% (w/v) trypsin (Worthington Biochemical, Lakewood, NJ), 0.016% (w/v) ethylene diamine tetraacetic acid (EDTA), and 1% (w/v) DNaseI (Sigma, St. Louis, MO). The cells were cultured at 37°C/5% CO₂ in glial medium, which consisted of Minimal Essential Medium (GIBCO) supplemented with 10% (v/v) horse serum, 0.7% (w/v) glucose, and 16 µg/mL gentamicin, and either passaged 1–3 times or cryopreserved for future use. To prepare neuronal cultures, the cerebral cortex of one P0 mouse pup was dissociated in PBS containing 0.025% (w/v) trypsin, 0.01% (w/v) EDTA and 0.5% (w/v) DNaseI. The dissociated cells were transfected with 2.0 µg GFP-tagged mouse neurofilament protein M cDNA expression construct [Yan et al., 2007] by electroporation using an Amaxa Nucleofector (Lonza, Walkersville, MD; program O-05) and the Amaxa Mouse Neuron Nucleofection kit (VPG-1001). The volume of the cell suspension was 100 µL and the cell density ranged from 4 × 10⁶ to 6 × 10⁶ cells/mL. The transfected cells were then diluted to a density of about 1 × 10⁵ cells/mL and plated onto glass-bottomed dishes that had been coated with poly-D-lysine (Sigma) and laminin (BD Biosciences, San Jose, CA). Glass coverslips bearing glia (>80% confluency) were suspended over the neurons using dots of paraffin wax as spacers, and the resulting sandwich cultures were maintained initially at 37°C/5% CO₂ in plating medium, which consisted of NeurobasalTM medium

(GIBCO Life Technologies) supplemented with 2% (v/v) B-27 Supplement Mixture (GIBCO Life Technologies), 0.27% glucose, 2 mM glutamine, 37.5 mM NaCl, 5% (v/v) fetal bovine serum (Thermo Scientific, Waltham, MA), 16 µg/mL gentamicin, and 2.5 µM cytosine arabinoside (Sigma). After two days, the plating medium was replaced with culturing medium, which was identical to the plating medium except that it lacked serum. Every four days, half the medium was removed and replaced with fresh medium.

Microscopy and Imaging

To observe neurofilament movement, cortical neuron axons were imaged after 8–12 days in culture by epifluorescence microscopy on a Nikon TE300 inverted microscope (Nikon, Garden City, NY) using a 100× Plan Apo VC 1.4NA oil immersion objective. The observation medium consisted of Hibernate-E (BrainBits, Springfield, IL) supplemented with 2% (v/v) B-27 Supplement Mixture, 0.3% (w/v) glucose, 1 mM L-glutamine, 37.5 mM NaCl, and 10 µg/mL gentamicin. The temperature on the microscope stage was maintained using an Air Stream incubator (Nevtek, Williamsville, VA). A layer of dimethylpolysiloxane fluid (Sigma, five centistokes) was floated over the observation medium to prevent evaporation. For time-lapse imaging, the exciting light from the mercury arc lamp was attenuated 12-fold using neutral density filters, and images were acquired with 1 s exposures at 5 s intervals using a Micromax 512BFT cooled CCD camera (Roper Scientific, Trenton, NJ) and MetaMorphTM software (Molecular Devices, Sunnyvale, CA). With a 100× objective, each pixel in the acquired images corresponded to a size of 0.13 µm × 0.13 µm. It was necessary to adjust the focus occasionally during movie acquisition to correct for focus drift.

Image Analysis

Neurofilaments in the time-lapse movies were selected for analysis if they were sufficiently bright and if they could be traced unambiguously from one end to the other without any overlap with other filaments. Filaments were excluded if they were out of focus in any of the frames of interest, or if there was bright or nonuniform fluorescence in the background. All quantification was carried out using MetaMorphTM image analysis software. We used the MetaMorphTM Linescan tool to obtain linear fluorescence intensity profiles along the filaments. The medial axis of each filament was traced manually in each image plane, extending ~10 pixels beyond the filament at either end (Fig. 1). The Linescan width was set to seven pixels (0.91 µm), which was sufficient to include >90% of the neurofilament fluorescence (data not shown). The average intensities in analog-to-digital units (ADU) were exported to Microsoft Excel for further analysis. To correct for background, each Linescan region was shifted horizontally

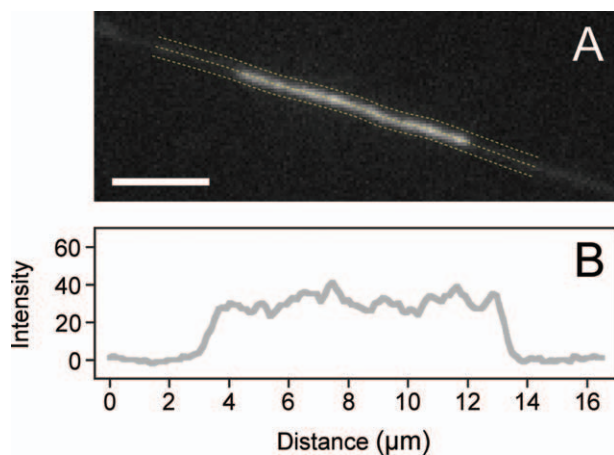


Fig. 1. Linear intensity profile along a neurofilament. **A.** Image of a short neurofilament obtained from a time-lapse movie of a cultured neuron expressing GFP-tagged neurofilament protein M. A line was drawn along the medial axis of the filament, extending into the background at both ends, using the Region tools in the MetaMorphTM software (central dashed yellow line). The intensity profile was obtained using the Linescan tool with a line width of 7 pixels (0.91 μm). The boundaries of the Linescan region are shown here by the upper and lower dashed yellow lines. Note that the filament is about 10 nm in diameter but it appears to be several hundred nanometers in width here because of diffraction blurring. Scale bar = 4 μm . **B.** Graph of the resulting linear fluorescence intensity profile. The intensity on the y -axis is the average intensity across the width of the Linescan region in arbitrary ADU. The nonuniformity along the filament probably reflects nonuniform (presumably random) incorporation of GFP-tagged neurofilament protein M fusion protein, though small kinks or undulations along the filament that are below the resolution limit could also contribute. Note that the fluorescence of the filament decays to background over several hundred nanometers at the filament ends because of diffraction blurring.

or vertically by 10 pixels (1.3 μm) to sample the background adjacent to the filament and then the average background intensity was subtracted from the filament intensity profile to generate a background-corrected intensity profile. To compare the fluorescence intensities of neurofilaments before, during, and after a folding event, we corrected the background-corrected fluorescence intensities for photobleaching using photobleaching calibration curves obtained from “reference” filaments that remained paused within the imaging area during the movies. For pseudocolor representations, we applied a standard rainbow color lookup table and then modulated the intensities of the pixels in the resulting color image to be proportional to their intensities in the original grayscale image [Brown et al., 1992; Hinman and Sammak, 1998].

We analyzed two types of events: “folding” events and “moving” events. An event was classified as a folding event if the filament exhibited a decrease in its apparent length accompanied by an increase in the fluorescence intensity along part or all of its length. The length was calculated as the axial distance between the two filament ends in the linear

intensity profile. The images of the filaments appear blurred because they are diffraction limited, so we defined the end of the filament as the point at which the fluorescence intensity decreased to half-height. Moving events were evident from the displacement of the filaments along the axon. For the present study, we only analyzed moving filaments that exhibited sustained movement in a single direction for a distance equal to at least the length of that filament. To determine the total intensity along all or part of a filament, we summed the intensity values along the corresponding portion of the filament in the background-corrected linear intensity profile.

Results

Live Imaging of Axonal Neurofilaments

To observe the folding behavior of neurofilaments, we transfected neonatal mouse cortical neurons with GFP-tagged mouse neurofilament protein M and then cultured the cells on glass coverslips using the glial sandwich technique of Kaech and Banker [2006]. Eight to twelve days later, after the cells had extended long axons, we observed the cultures by time-lapse fluorescence microscopy. We have shown previously that the GFP-tagged neurofilament protein M becomes incorporated throughout all neurofilaments in these neonatal cultures and that many of the axons contain relatively few neurofilaments, which makes them particularly suitable for tracking the movements of these polymers [Wang and Brown, 2010].

Neurofilaments are Very Flexible

Biophysical studies on neurofilaments *in vitro* have demonstrated that these polymers are remarkably flexible, with persistence lengths on the order of several hundred nanometers [Dalhaimer et al., 2005; Wagner et al., 2007; Beck et al., 2010] (Table I). In cultured neurons, this flexibility is most clearly evident in broader regions of the axons such as in growth cones [Uchida and Brown, 2004] and at branch points, where neurofilaments often fold or loop back on themselves in a variety of configurations. An example of this is shown in Fig. 2, which shows an isolated neurofilament that appears to be trapped at an axon branch point (Supporting Information Movie 1). The breadth of the axon at this location allows the configuration of the filament to be resolved. The filament writhes dynamically over a period of many minutes, at one point appearing to become contorted into a pretzel-shaped knot, and at a later point folding back onto itself to form a hairpin loop. Areas of overlap result in an increase in brightness even when the two overlapping segments cannot be discerned.

Neurofilaments Frequently Fold and Unfold Along Their Length

The flexibility of axonal neurofilaments is also evident within the axon shaft, where we frequently observe

Table I. The Persistence Lengths of Various Biological Polymers

Polymer	Persistence length (nm)	Reference
DNA	45	Bednar et al. [1995]
Neurofilaments	125	Beck et al. [2010]
Microfilaments	18,000	Gittes et al. [1993]
Microtubules	5,200,000	Gittes et al. [1993]

The persistence length of a polymer is the minimum length over which thermal bending becomes appreciable, and it is directly proportional to the flexural rigidity [Boal, 2012]. Note the remarkable flexibility of neurofilaments, which approaches that of DNA. In contrast, microtubules and microfilaments are relatively stiff.

neurofilaments fold and unfold along all or part of their length. These folds can occur at any point along the length of the filaments, either internally or at the ends. The precise configuration of these folds cannot be resolved because the filaments are constrained by the narrow width of the axons, which are typically just tenths of a micrometer in diameter. However, the folding is evident from the increase in the brightness of the filament at the site of the fold, accompanied by a corresponding decrease in the apparent filament length. Figure 3 shows an example of a pausing neurofilament which folds and then unfolds at one end over the course of 110 s (Supporting Information Movie 2).

Analysis of Neurofilament Folding

To analyze neurofilament folding quantitatively, we examined a total of 52 time-lapse movies, each 15 min in length (total number of moving filaments = 92), and looked for isolated axonal neurofilaments that exhibited folding behavior. In total, we identified 14 folding events that met our analysis criteria for focus, brightness, lack of overlap with other filaments, traceability and clean background (see Methods). In four of these cases, the filament folded up along its entire length, in six of the cases, the fold was localized at one end of the filament, and in the remaining four of the cases, the fold was localized internally, away from the ends. Though we cannot be sure, it seems likely that these folds are caused either by the filaments folding back on themselves along all or part of their length in a single or double hairpin configuration, or by the filaments becoming compressed along all or part of their length into a concertina-like configuration (Fig. 4).

To analyze the length and intensity of the filaments during folding, we identified 10 filaments that were observed to fold and then unfold. All of these filaments were suitable for length measurements, and eight of them were also suitable for intensity measurements. Figure 5 shows three examples, including two filaments that folded at or close to their ends (Figs. 5A and 5B) and one that folded along its entire length (Fig. 5C), and Fig. 6 shows the average measurements for all 10 filaments. Note that

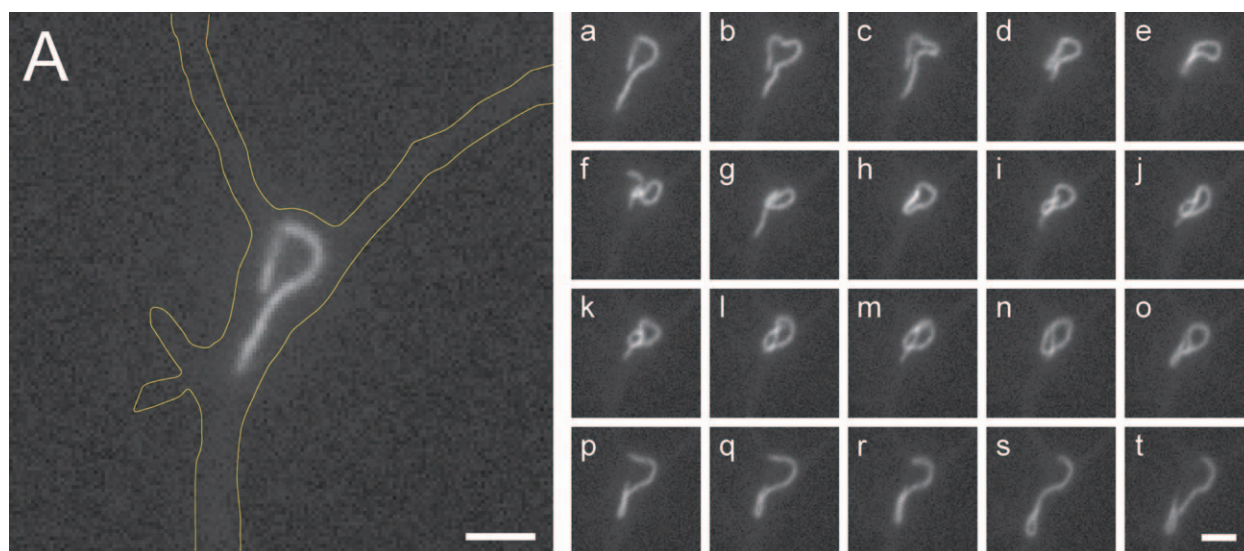


Fig. 2. Neurofilaments are flexible. **A.** Image of a neurofilament trapped at an axon branch point. The location of the axon is indicated by the yellow lines (note that these lines are drawn outside the boundaries of the axon to avoid obscuring the filament). **a–t.** Selected frames from a time-lapse movie showing the contortions of the filament over a time period of 515 s. The filament writhes dynamically, becoming contorted into a tight pretzel-shaped knot at one point, and folding back onto itself to form a hairpin loop at a later point. Note that when the filament folds back on itself the region of overlap can be distinguished by a local increase in the fluorescence intensity even though the two overlapping segments cannot be resolved. The motion of this filament may reflect the direct action of molecular motors, but we believe that it is more likely to be indirect, due to jostling by moving organelles. Proximal is bottom, distal is top. Scale bars = 2.5 μ m. See Supporting Information Movie 1.

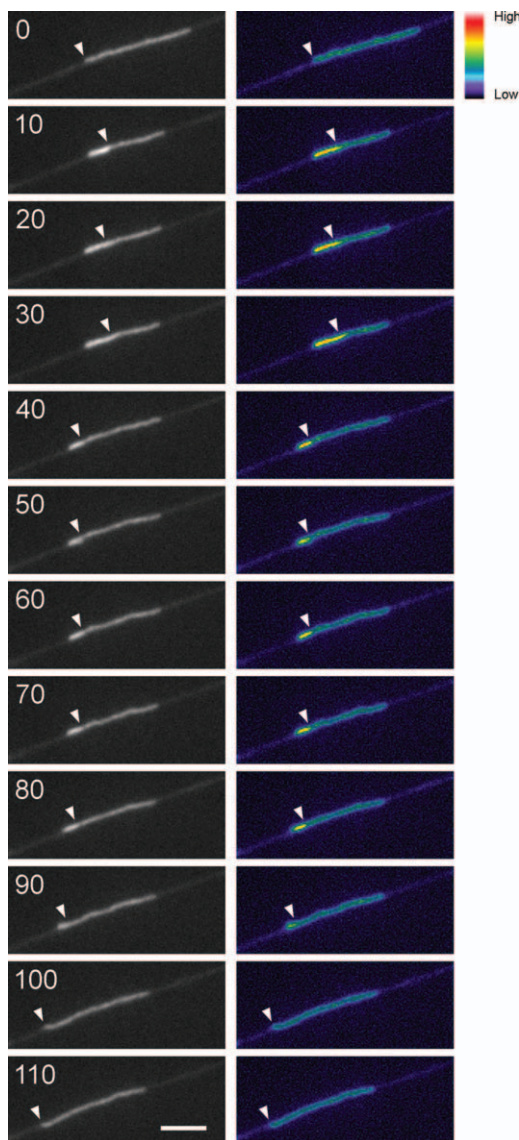


Fig. 3. Folding and unfolding behavior of a pausing neurofilament. Left: selected frames from a time-lapse movie demonstrating the folding and unfolding of a neurofilament in an axon over a period of 110 s. Right: the same images displayed with intensity-modulated pseudocolor (see Methods). The white arrowheads mark the apparent location of the proximal end of the filament, which appears to fold back on itself to form a hairpin loop (this configuration is more evident in the accompanying movie, particularly when the filament is unfolding). The folding is evident from the local increase in brightness of the filament at one end and the corresponding decrease in the apparent filament length. Note that the length of the filament is the same at the start and end of this sequence. Note also that the filament inches towards the left during this sequence because the initial folding event is accompanied by a retraction of the right end of the filament and then the later unfolding event is accompanied by an extension of the left end. Folding behavior such as this is fairly common in our movies. Proximal is left, distal is right. Scale bar = 4 μm . See Supporting Information Movie 2.

folding is accompanied by an apparent decrease in filament length, but our measurements before and after folding indicate that both length and intensity are conserved (Fig. 6).

To analyze the extent of folding, we quantified the average fluorescence intensity in each folded region and expressed it as a ratio of the average fluorescence intensity of the same filament in the unfolded configuration. On average, the intensity of the neurofilament fluorescence increased by 2.3-fold within the folded region (minimum = 1.9-fold, maximum = 3.2-fold, $n = 14$). Filaments that folded at their ends or along their entire length tended to have a lower increase in fluorescence (average = 2.2-fold, $n = 10$) compared to those that folded internally (average = 2.6-fold, $n = 4$). This could be explained by a higher incidence of double hairpin folds internally and a higher incidence of single hairpin folds at filament ends, though it is also possible that this range of fluorescence intensities could be explained by concertina folds with undulations of differing amplitude and frequency (Fig. 4).

Neurofilaments Move in an Unfolded, that is, Fully Extended, Configuration

Given the flexibility of neurofilaments evident in the above analyses, we would expect that neurofilaments might also sometimes move in a folded configuration. However, in more than 10 years of tracking neurofilament movement in axons, we are struck by the fact that this does not appear to be the case. Though neurofilaments exhibit short-range movements when they are folding and unfolding, when they move in a sustained manner, the fluorescence intensity invariably appears relatively uniform along their entire length, suggesting that the filaments move in a fully extended configuration (Fig. 7 and Supporting Information Movie 3). Given that neurofilament

A. Hairpin fold



B. Double hairpin fold



C. Terminal concertina fold



D. Internal concertina fold



Fig. 4. Simulation of various possible folding configurations. A. A single hairpin fold. B. A double hairpin fold. C. A terminal concertina fold (i.e., at the end of a filament). D. An internal concertina fold (i.e., away from the ends). The expected increase in fluorescence intensity within the folded region is twofold for a single hairpin fold and threefold for a double hairpin fold. In the case of concertina folds, the expected increase in fluorescence intensity depends on the amplitude and frequency of the undulations.

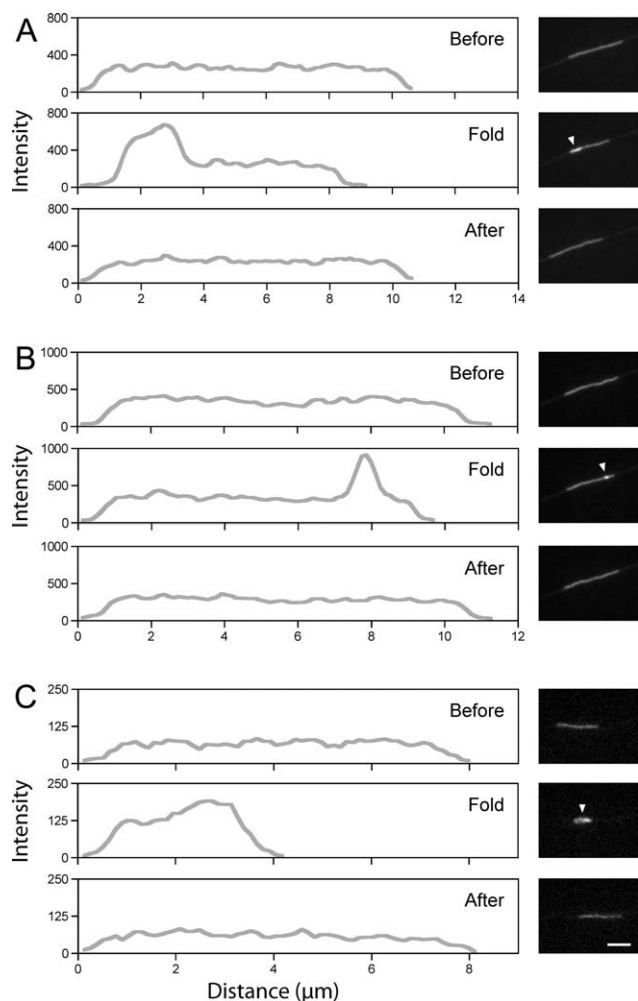


Fig. 5. Linear intensity profile analysis of folding filaments. Three examples of filaments that were observed to fold and then unfold. The images of the filaments are shown on the right and the linear intensity profiles are shown on the left. The fluorescence intensity on the *y*-axis is in arbitrary ADU. The distance on the *x*-axis is measured from the proximal (left) end of the filament. In each case, the folding event is accompanied by a decrease in the apparent length of the filament and a corresponding increase in the fluorescence intensity at the site of the fold (white arrowheads on images), but note that the length and the intensity of the filaments before and after the folding event are comparable. The filaments in A and B fold along part of their length, whereas the filament in C folds up along its entire length. Proximal is left, distal is right. Scale bar = 4 μm .

folding results in a twofold to threefold increase in the fluorescence intensity (see above), and given the absence of any such peaks in the linear fluorescence intensity profiles, it is clear from these data that the filaments move in an entirely unfolded configuration. Thus, neurofilament folding occurs when the filaments are not undergoing sustained movement, and folded filaments invariably appear to straighten out when they move. Examples of this behavior can be seen in Supporting Information Movies 4–7.

To analyze the uniformity of the fluorescence intensity along moving neurofilaments quantitatively, we obtained

linear fluorescence intensity profiles for 50 moving filaments. For these analyses, we only selected filaments that were undergoing bouts of sustained unidirectional movement (see Materials and Methods section). We divided each filament into three contiguous segments of equal length (leading, middle, and trailing) and measured the fluorescence intensities within each of these regions. On average, the fluorescence intensity of the leading segment (i.e., at the front of the moving filament) was not significantly different from the middle or trailing segments (average intensity ratio = 1.0 ± 0.13 for both) and the trailing segment was not significantly different from the middle segment (average intensity ratio = 1.0 ± 0.1) (Figs. 8A–8C; $P > 0.9$, Wilcoxon test, $n = 50$). To address the possibility of small hairpin or concertina folds at the leading ends of the moving filaments, we measured the fluorescence intensities within a short region (10 pixels; 1.3 μm) at the tip of each moving filament and compared these intensities to the average intensity along the rest of the filament, but again there was no significant difference (average intensity ratio = 1.0 ± 0.13 ; Fig. 8D; $P > 0.5$, Wilcoxon test, $n = 39$).

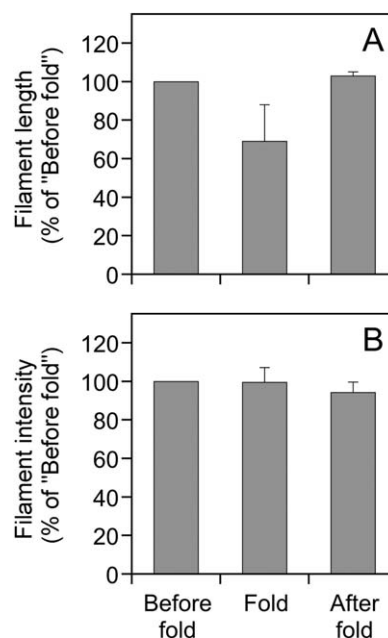


Fig. 6. Length and intensity are conserved when neurofilaments fold. **A.** Average relative filament length before, during, and after a folding event ($n = 10$). For each filament, the lengths before, during, and after the fold were normalized to the length before the fold. The apparent length of the filaments decreases during folding but returns to the original length after unfolding. The length of the folded filaments is highly variable because it depends on the configuration and extent of the fold. **B.** Average relative fluorescence intensity of filaments before, during, and after a folding event ($n = 8$). For each filament, the fluorescence intensities before, during, and after the fold were corrected for photobleaching and then normalized to the fluorescence intensity before the fold. The error bars in both graphs represent the standard deviation about the mean. Note that both the length and intensity of the filaments are conserved during the folding process.

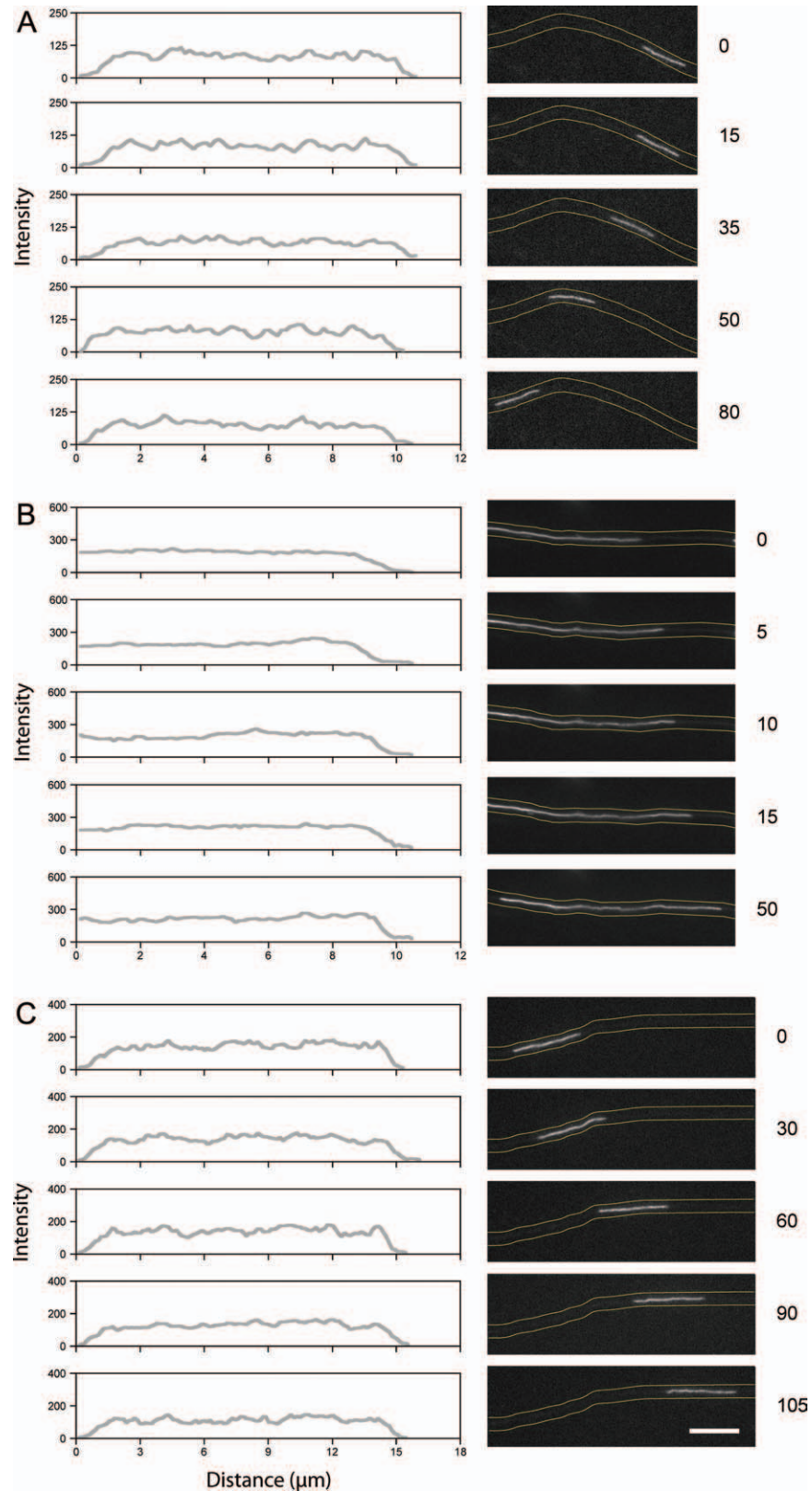


Fig. 7. Linear intensity profile analysis of moving filaments. **A.** A retrogradely moving neurofilament. **B** and **C.** Two anterogradely moving neurofilaments. Right: selected images from the time-lapse movies. The time intervals in seconds are shown on the far right. The location of the axon is indicated by the parallel yellow lines (note that these lines are drawn outside the boundaries of the axon to avoid obscuring the filament). Left: the corresponding linear fluorescence intensity profiles. The fluorescence intensity on the y -axis is in arbitrary ADU. The distance on the x -axis is measured from the proximal (left) end of the filament in A and C. Due to the long length of the filament in B, only the leading 10 μm of this filament is represented in the linear fluorescence intensity profile. The leading end of the filament is on the left in A (filament moving in the retrograde direction) and on the right in B and C (filaments moving in the anterograde direction). Note the uniform fluorescence intensity along the length of each filament, extending all the way to the leading end, which indicates that the filaments are moving in an unfolded (i.e., fully extended) configuration. Proximal is left, distal is right. Scale bar = 10 μm . The filament in C can be seen in Supporting Information Movie 3.

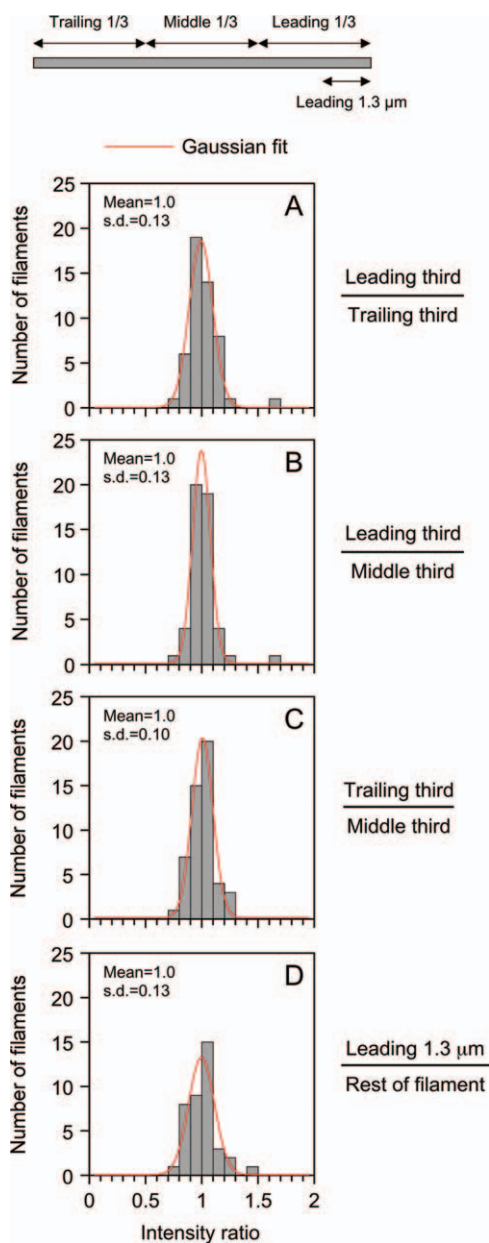


Fig. 8. The fluorescence intensity is uniform along the length of moving neurofilaments. The fluorescence intensities of moving neurofilaments were quantified in order to reveal the presence of any folds. **A–C.** Data for 50 neurofilaments (average length = 7.8 μm , minimum = 1.8 μm , maximum = 19.3 μm). Each neurofilament was split into thirds by length. The intensity ratio is the average intensity in one region (leading, middle, or trailing third) relative to another. **D.** Data for 39 neurofilaments that exceeded 3.9 μm in length (average length = 9.2 μm , minimum = 3.9 μm , maximum = 19.3 μm). Here, the intensity ratio is the average intensity in the leading 1.3 μm (10 pixels) of each filament to the average intensity of the remaining length. For each comparison, there was no statistically significant difference between the intensity ratio distributions and a Gaussian distribution with a mean of 1.0 (red line; $P > 0.1$, one-sample Kolmogorov-Smirnov test for goodness of fit).

Discussion

Neurofilaments are unique among the known cargoes of axonal transport in that they are flexible protein polymers, just 10 nm in diameter, that can be tens of micrometers in length. In the present study, we show that these flexible polymers frequently exhibit complex and reversible folding behaviors in axons. When this occurs within the narrow confines of the axon of a cultured neuron, we find that the folding can be detected by an increase in the fluorescence intensity at that location even though the precise configuration of the fold cannot be resolved. Remarkably, however, when neurofilaments move in a sustained manner they straighten out and exhibit relatively uniform fluorescence along their length with no evidence of any folding, even at the extreme tip of their leading ends. Thus, neurofilaments appear to be transported in an unfolded, that is, fully extended, configuration.

We are intrigued by the question of how a long polymer as flexible as a neurofilament could move through axonal cytoplasm in an extended configuration. A macroscopic analogy could be the movement of a piece of cooked spaghetti through a viscous medium. Clearly, it would not be possible to push the spaghetti from the middle or rear while keeping the spaghetti in an extended configuration. Thus, if a motor binds to a neurofilament at some location away from the filament ends, the neurofilament might be expected to be pulled forward with the free ends folding back on themselves to form a hairpin fold at the leading end of the moving filament. Indeed, such folding is common in our movies and is easy to detect because it results in a twofold increase in the filament intensity at that location. The fact that we do not observe any intensity increase at the leading ends of moving neurofilaments indicates that these ends are not folded. Thus, we speculate that neurofilaments are pulled from their leading ends, which implies that there are always motors at or close to the leading ends of these polymers when they are moving.

There are two possible mechanisms by which cells could ensure that there is always a motor at the leading end of moving neurofilaments (Fig. 9). The first is that the motors bind randomly along the length of the filament, but at such a high density that there is a high probability of finding a motor very close to the ends of the polymer. Based on the length and flexibility of neurofilaments, this random binding model would require that many motors attach to each moving filament in order to ensure that there is no folding during movement. There is evidence from atomic force and immunogold electron microscopy that dynein may bind at multiple sites along the length of neurofilaments in vitro [Shah et al., 2000; Wagner et al., 2003] so perhaps such a model is not far-fetched. However, it is not clear how the activities of these motors would be coordinated. The second possible

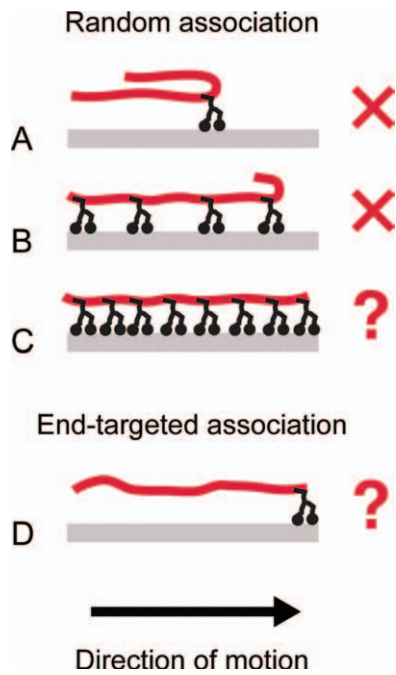


Fig. 9. Some possible modes of motor association with moving neurofilaments. **A.** If a single motor binds at a random location along a filament, then the moving filament will assume a hairpin fold at its leading end. The length of the fold will be dependent on the site of motor attachment. **B.** If several motors bind at random locations along the length of a filament, then the length of the hairpin fold at the leading end of the moving filament will tend to be shorter because the average distance of the leading end from the nearest motor will be less. **C.** If the motor density is high enough, random binding could, in theory, always result in at least one motor close to the leading end of the filament without the need for an end-targeting mechanism. **D.** An alternative model which ensures that there is a motor at the leading end of all moving filaments, even at low motor densities, is to target motors to neurofilament ends, allowing a single motor to pull a neurofilament in a fully extended configuration with no folding. The unfolded configuration of moving neurofilaments appears to be inconsistent with random association at low or medium motor densities (A,B), leaving us with two possibilities: a high density of randomly associated motors along each filament (C), or targeted association of motors with the leading ends of moving filaments (D). Either possibility has intriguing implications for the mechanisms of the motor-cargo interaction.

mechanism is that the neurofilament motors somehow bind preferentially to the ends of axonal neurofilaments.

Selective recruitment of motors to the ends of cytoskeletal polymers has been described for microtubules but not for intermediate filaments. In the case of microtubules, this recruitment is mediated by microtubule plus-end tracking proteins which bind to the growing plus ends of these dynamic cytoskeletal polymers [Gouveia and Akhmanova, 2010]. The targeting mechanism is thought to involve the GTP cap of the growing microtubule or some unique structural feature of growing ends. However, this mechanism cannot apply to intermediate filaments because they have very distinct assembly dynamics from

microtubules [Ngai et al., 1990; Coleman and Lazarides, 1992; Vikstrom et al., 1992; Colakoglu and Brown, 2009] and they have no structural polarity [Herrmann and Aebi, 2004]. Moreover, because of the lack of structural polarity, both ends of these polymers are presumed to be identical so any motor that bound to one end might also bind to the other end too. If a motor bound to just one end, that end would become the leading end with the filament in tow. However, if motors bound to both ends, would the motors engage in a tug-of-war or would their activity have to be somehow coordinated to ensure directed motion?

Clearly, a critical test of the random and end-targeted motor binding models shown in Fig. 9 will be to determine the density and location of kinesin and dynein motors on moving neurofilaments in vivo. One theoretical estimate suggests that a single dynein or kinesin motor may be sufficient to move a single neurofilament in axons [Mitchell and Lee, 2009], but this calculation assumed an average neurofilament length of 1.8 μm , which is much shorter than observed experimentally, and also relied on unverified assumptions about the viscous drag acting on neurofilaments in axons. Nevertheless, force measurements in vivo indicate that a single motor is sufficient to move lipid droplets, which are considerably larger than neurofilaments [Shubeita et al., 2008], so it seems reasonable to assume that a single motor could also move a single neurofilament. Our present observations would suggest that if this is the case, that motor might have to be bound to one end of the neurofilament, and that this would become the leading end when the filament moved.

While it is clear that sustained anterograde and retrograde neurofilament movement in axons reflects the direct action of microtubule motors, the forces that cause neurofilaments to fold and unfold when they are pausing are not clear. One possibility is that folding and unfolding also reflect the direct actions of bound motors. For example, if multiple motors bind along the length of a neurofilament, folding could arise when these motors act individually or in an uncoordinated manner. However, the fact that such folding behavior only occurs when neurofilaments are pausing indicates that such movements are always short-range and never become sustained. Another possibility is that folding could be an indirect result of the movement of other cargoes, such as membranous organelles or other cytoskeletal polymers, which might transiently bind or snag a portion of a neurofilament as they brush by, effectively tugging the polymer into a fold. Thus, the short-range movements of neurofilaments that cause them to fold and unfold in axons might not necessarily reflect the direct actions of motors on these polymers. To resolve this question, it will be necessary to perform a more detailed analysis of neurofilament folding with higher temporal and spatial resolution than we employed in the current study, and to develop methods to

measure directly the forces acting on these polymers in axons.

Acknowledgments

We thank Roy Beck for helpful discussions. This project was funded by NSF grant IOS-0818653 and NIH grant R01-NS38526, with additional support provided by NIH grant P30-NS045758. N.J.T. was supported by an NSF Research Experiences for Undergraduates supplement to grant IOS-0818653 and a Michael Grever Internship from the Ohio State University College of Medicine. The authors declare no competing financial interests.

References

- Beck R, Deek J, Choi MC, Ikawa T, Watanabe O, Frey E, Pincus P, Safinya CR. 2010. Unconventional salt trend from soft to stiff in single neurofilament biopolymers. *Langmuir* 26:18595–18599.
- Bednar J, Furrer P, Katritch V, Stasiak AZ, Dubochet J, Stasiak A. 1995. Determination of DNA persistence length by cryo-electron microscopy. Separation of the static and dynamic contributions to the apparent persistence length of DNA. *J Mol Biol* 254:579–594.
- Boal DH. 2012. *Mechanics of the Cell*. New York: Cambridge University Press. 608 p.
- Brown A. 2000. Slow axonal transport: stop and go traffic in the axon. *Nat Rev Mol Cell Biol* 1:153–156.
- Brown A, Slaughter TS, Black MM. 1992. Newly assembled microtubules are concentrated in the proximal and distal regions of growing axons. *J Cell Biol* 119:867–882.
- Colakoglu G, Brown A. 2009. Intermediate filaments exchange subunits along their length and elongate by end-to-end annealing. *J Cell Biol* 185:769–777.
- Coleman TR, Lazarides E. 1992. Continuous growth of vimentin filaments in mouse fibroblasts. *J Cell Sci* 103 (Pt 3):689–698.
- Dalhaimer P, Wagner OI, Leterrier J-F, Janmey PA, Aranda-Espinoza H, Discher DE. 2005. Flexibility transitions and looped adsorption of wormlike chains. *J Polym Sci Part B: Polym Phys* 43:280–286.
- Francis F, Roy S, Brady ST, Black MM. 2005. Transport of neurofilaments in growing axons requires microtubules but not actin filaments. *J Neurosci Res* 79:442–450.
- Gittes F, Mickey B, Nettleton J, Howard J. 1993. Flexural rigidity of microtubules and actin filaments measured from thermal fluctuations in shape. *J Cell Biol* 120:923–934.
- Gouveia SM, Akhmanova A. 2010. Cell and molecular biology of microtubule plus end tracking proteins: end binding proteins and their partners. *Int Rev Cell Mol Biol* 285:1–74.
- He Y, Francis F, Myers KA, Yu W, Black MM, Baas PW. 2005. Role of cytoplasmic dynein in the axonal transport of microtubules and neurofilaments. *J Cell Biol* 168:697–703.
- Helfand BT, Loomis P, Yoon M, Goldman RD. 2003. Rapid transport of neural intermediate filament protein. *J Cell Sci* 116:2345–2359.
- Herrmann H, Aebi U. 2004. Intermediate filaments: molecular structure, assembly mechanism, and integration into functionally distinct intracellular scaffolds. *Annu Rev Biochem* 73:749–789.
- Hinman LE, Sammak PJ. 1998. Intensity modulation of pseudocolor images. *Biotechniques* 25:124–128.
- Jung C, Lee S, Ortiz D, Zhu Q, Julien JP, Shea TB. 2005. The high and middle molecular weight neurofilament subunits regulate the association of neurofilaments with kinesin: inhibition by phosphorylation of the high molecular weight subunit. *Brain Res Mol Brain Res* 141:151–155.
- Kaech S, Banker G. 2006. Culturing hippocampal neurons. *Nat Protocols* 1:2406–2415.
- Lasek RJ, Paggi P, Katz MJ. 1992. Slow axonal transport mechanisms move neurofilaments relentlessly in mouse optic axons. *J Cell Biol* 117:607–616.
- Mitchell CS, Lee RH. 2009. A quantitative examination of the role of cargo-exerted forces in axonal transport. *J Theoret Biol* 257:430–437.
- Ngai J, Coleman TR, Lazarides E. 1990. Localization of newly synthesized vimentin subunits reveals a novel mechanism of intermediate filament assembly. *Cell* 60:415–427.
- Perrot R, Berges R, Bocquet A, Eyer J. 2008. Review of the multiple aspects of neurofilament functions, and their possible contribution to neurodegeneration. *Mol Neurobiol* 38:27–65.
- Prahlad V, Helfand BT, Langford GM, Vale RD, Goldman RD. 2000. Fast transport of neurofilament protein along microtubules in squid axoplasm. *J Cell Sci* 113:3939–3946.
- Shah JV, Flanagan LA, Janmey PA, Leterrier J-F. 2000. Bidirectional translocation of neurofilaments along microtubules mediated in part by dynein/dynactin. *Mol Biol Cell* 11:3495–3508.
- Shubeita GT, Tran SL, Xu J, Vershinin M, Cermelli S, Cotton SL, Welte MA, Gross SP. 2008. Consequences of motor copy number on the intracellular transport of kinesin-1-driven lipid droplets. *Cell* 135:1098–1107.
- Uchida A, Brown A. 2004. Arrival, reversal and departure of neurofilaments at the tips of growing axons. *Mol Biol Cell* 15:4215–4225.
- Uchida A, Alami NH, Brown A. 2009. Tight functional coupling of kinesin-1A and dynein motors in the bidirectional transport of neurofilaments. *Mol Biol Cell* 20:4997–5006.
- Vikstrom KL, Lim S-S, Goldman RD, Borisy GG. 1992. Steady state dynamics of intermediate filament networks. *J Cell Biol* 118:121–129.
- Wagner OI, Lifshitz J, Janmey PA, Linden M, McIntosh TK, Leterrier JF. 2003. Mechanisms of mitochondria-neurofilament interactions. *J Neurosci* 23:9046–9058.
- Wagner OI, Ascano J, Tokito M, Leterrier JF, Janmey PA, Holzbaur EL. 2004. The interaction of neurofilaments with the microtubule motor cytoplasmic dynein. *Mol Biol Cell* 15:5092–5100.
- Wagner OI, Rammensee S, Korde N, Wen Q, Leterrier JF, Janmey PA. 2007. Softness, strength and self-repair in intermediate filament networks. *Exp Cell Res* 313:2228–2235.
- Wang L, Brown A. 2010. A hereditary spastic paraplegia mutation in kinesin-1A/KIF5A disrupts neurofilament transport. *Mol Neurodegener* 5:52.
- Wang L, Ho C-L, Sun D, Liem RKH, Brown A. 2000. Rapid movement of axonal neurofilaments interrupted by prolonged pauses. *Nat Cell Biol* 2:137–141.
- Xia CH, Roberts EA, Her LS, Liu X, Williams DS, Cleveland DW, Goldstein LS. 2003. Abnormal neurofilament transport caused by targeted disruption of neuronal kinesin heavy chain KIF5A. *J Cell Biol* 161:55–66.
- Yabe JT, Jung CW, Chan WKH, Shea TB. 2000. Phospho-dependent association of neurofilament proteins with kinesin in situ. *Cell Motil Cytoskeleton* 45:249–262.
- Yan Y, Jensen K, Brown A. 2007. The polypeptide composition of moving and stationary neurofilaments in cultured sympathetic neurons. *Cell Motil Cytoskeleton* 64:299–309.